



A new organic far-red mechanofluorochromic compound derived from cyano-substituted diarylethene

Xiqi Zhang ^{a,*}, Zhiyong Ma ^b, Meiyang Liu ^c, Xiaoyong Zhang ^a, Xinru Jia ^b, Yen Wei ^{a,*}

^a Department of Chemistry and the Tsinghua Center for Frontier Polymer Research, Tsinghua University, Beijing 100084, China

^b Beijing National Laboratory for Molecular Sciences, Key Laboratory of Polymer Chemistry and Physics of the Ministry of Education, College of Chemistry and Molecular Engineering, Peking University, Beijing 100871, China

^c Beijing National Laboratory for Molecular Sciences (BNLMS), Key Laboratory of Organic Solids, Laboratory of New Materials, Institute of Chemistry, Chinese Academy of Sciences, Beijing 100190, China

ARTICLE INFO

Article history:

Received 28 August 2013

Received in revised form 30 September 2013

Accepted 14 October 2013

Available online 25 October 2013

Keywords:

Far-red fluorescence

Mechanofluorochromic compound

Cyano-substituted diarylethene derivative

Mechanism

ABSTRACT

A new cyano-substituted diarylethene derivative (**R-NH₂**) with reversible far-red mechanofluorochromic property was synthesized and confirmed by standard spectroscopic methods. To the best of our knowledge, the 684 nm red-shifted wavelength of the ground **R-NH₂** is the longest wavelength that has appeared in the literature. The mechanofluorochromic mechanism was investigated by small and wide-angle X-ray scattering and was ascribed to the destruction of crystalline structure. More in-depth study by infrared spectra and time-resolved emission-decay behaviors showed that the changes of C–H out-of-plane bending vibrations in aryl group of the compound and the obvious increase of fluorescence lifetime might be the fundamental reasons. The synthetic strategy reported here can be extended to prepare more and more long-wavelength emission mechanofluorochromic materials, which can broaden the scope of application of such materials and for thoroughly understanding the mechanofluorochromic mechanism.

© 2013 Elsevier Ltd. All rights reserved.

1. Introduction

Mechanofluorochromic materials have advanced fluorescent properties that change in response to external force stimuli and expected to generate new intelligent materials based on their superior high efficiency and reproducibility compared with conventional fluorescent materials, and have got wide applications in sensors, memory chips, and security inks.^{1,2} Chemical structure and molecular assembly structure changes are considered as two major mechanofluorochromic ways. Between them, molecular assembly structure change is believed easier to realize the dynamic control of fluorescent process. In 2002, Weder et al. reported on two cyano-substituted diphenylethene derivatives-doped linear low-density polyethylene as the first two mechanofluorochromic materials.³ Since then, the appeared organic mechanofluorochromic materials were still extremely rare until 2010 due to the lack of established property–structure relationship.^{4–8} In 2010, Xu et al. reported on a compound derived from tetraphenylethylene and divinylanthracene, which exhibited obvious mechanofluorochromic and aggregation-induced emission (AIE) properties.⁹ The

unique AIE materials have attracted great research interest because they could overcome the notorious issues in most planar conjugated organic dyes named aggregation-caused quenching (ACQ) effect. Different AIE architectural frameworks involving siloles, triphenylethene, tetraphenylethene, distyrylanthracene, cyano-substituted diarylethene derivatives conjugated molecules have been developed and utilized for chemosensor and bioimaging applications.^{10–30}

Since 2010, the Xu's group synthesized and reported a number of new mechanofluorochromic compounds with AIE feature,^{31–37} and proposed a ‘molecular conformational planarization’ mechanism for mechanofluorochromic compounds to establish a common structure–property relationship of the mechanofluorochromic materials and AIE materials, which would be helpful in identifying and synthesizing more novel mechanofluorochromic materials.¹ According to this relationship, a number of new organic mechanochromic fluorescent compounds were synthesized, which greatly broadened the field of mechanofluorochromic materials.^{38–56} In view of this situation, the very critical thing is either to discover new structures of mechanofluorochromic materials or to broaden the range of the fluorescent emission wavelength. Among the existing reported mechanofluorochromic materials, the fluorescent emission of them mainly located at short wavelength from blue to yellow due to their inherent conjugated groups. Rare

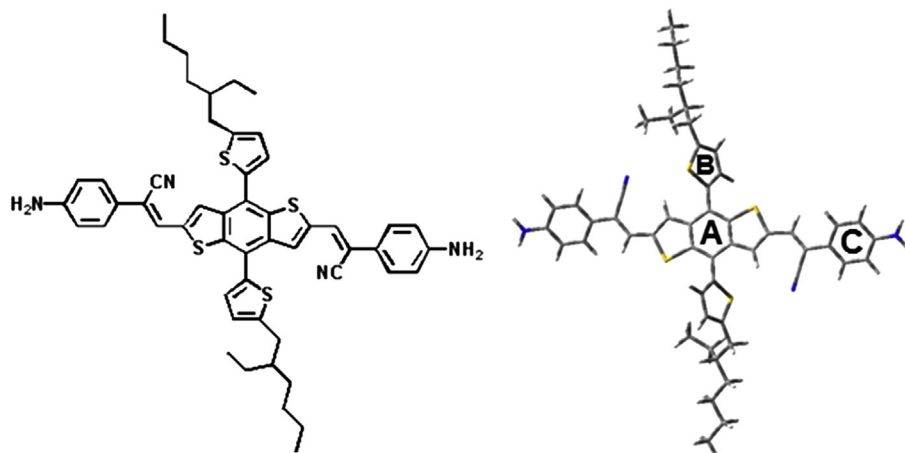
* Corresponding authors. E-mail addresses: sychyzhang@126.com (X. Zhang), weiyen@tsinghua.edu.cn (Y. Wei).

mechanofluorochromic materials emit fluorescence with longer wavelength. Although Ooyama et al. reported on a dye **SO₂** with red (625 nm) mechanofluorochromic property, only a 7 nm redshift was observed for the fluorescent emission wavelength after grinding the as-recrystallized dyes **SO₂**.⁵⁷

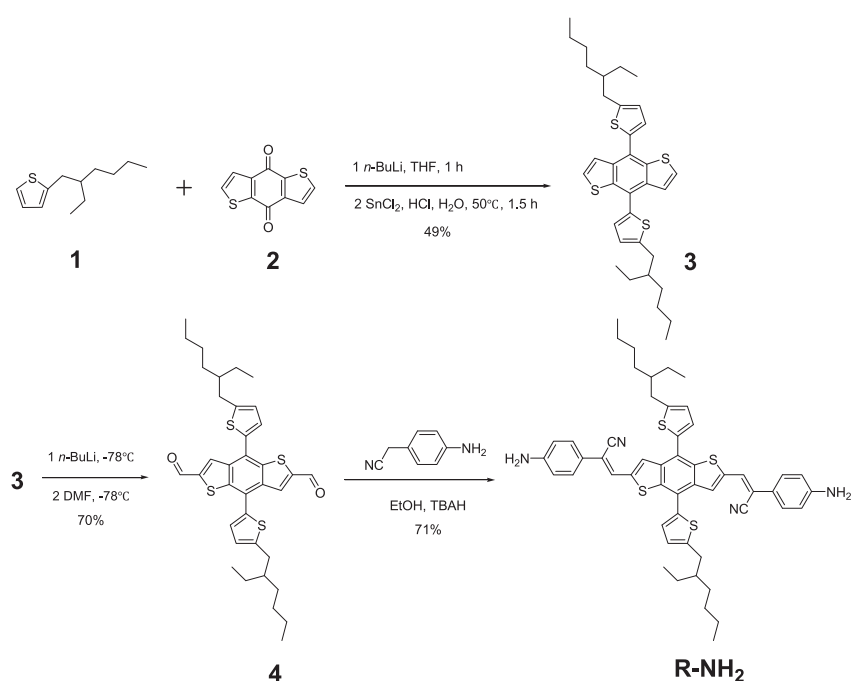
Herein, we report a new organic far-red fluorescent cyanosubstituted diarylethene-based compound (**R-NH₂**) (derivatized from 4, 8-bis[5-(2-ethylhexyl)-2-thienyl]benzodithiophene core structure with bis[2-(4-aminophenyl)acrylonitrile] side chains) with reversible mechanofluorochromic property (Scheme 1). Solid-state fluorescent spectra and UV-vis spectra were studied to reveal the mechanofluorochromic property. Then, the mechanofluorochromic mechanism was investigated by differential scanning calorimetry (DSC), infrared spectra (IR), small and wide-angle X-ray scattering (SWAXS), and time-resolved emission-decay behaviors.

2. Results and discussion

The fluorogen **R-NH₂** was prepared following the synthetic route shown in Scheme 2. Its structure was characterized and confirmed by standard spectroscopic methods. To gain the lowest energy spatial conformation of the compound, we conducted quantum mechanical computations by using the Gaussian 03 software.⁵⁸ The HOMO and LUMO of **R-NH₂** were obtained (Fig. 1) according to the density functional method at the B3LYP/6-31 G level after the structural optimization. The HOMO of the compound showed dispersed electron cloud distributions on all of the aryl groups and amino groups on the molecule, whereas the electron cloud of the LUMO exhibited the migration from both ends of the amino and thienyl groups to aryl core and cyano groups. Moreover, the compound adopted a twisted spatial conformation, as shown in the optimized structure (Scheme 1, right). The dihedral angles of



Scheme 1. The chemical structure (left) and the optimization geometry (right) of **R-NH₂**.



Scheme 2. Synthetic route of **R-NH₂**.

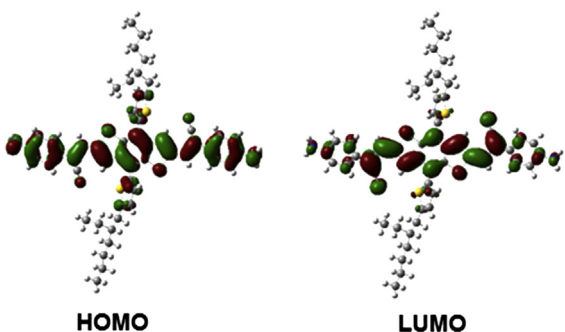


Fig. 1. Calculated spatial electron distributions of HOMO and LUMO of **R-NH₂**.

the adjacent aryl planes were calculated as 52° and 28° for planes A–B and A–C, respectively. While this twisted conformation may bring about mechanofluorochromism to the compound.¹

Therefore we ground the compound in a mortar with a pestle directly, the color of the compound was changed from bright red to dark brown immediately (**Fig. 2B**), meanwhile, the fluorescent light tuned from blood-red into dark red under 365 nm UV light (**Fig. 2A**), which showed obvious mechanofluorochromism. To quantitatively measure the fluorescent wavelength change of **R-NH₂** after

grinding, solid-state fluorescent spectra of the compound in original and grinding states were carried out, which realized a redshift of 24 nm from 660 nm in the original state to 684 nm in the grinding state (**Fig. 2C**). To the best of our knowledge, the redshifted wavelength at 684 nm is so far the longest wavelength that has appeared in the literature. The absolute fluorescent quantum yield for the original and ground samples were determined as 3.4% and 1.6%, respectively. The solid-state UV–vis spectra also revealed the change before and after grinding the sample, which was shown in **Fig. 2D**. As the original sample was ground, the absorption area ranging from 600 to 800 nm significantly increased, causing prodigious changes in the color of the sample. This result demonstrated that **R-NH₂** is also a mechanochromic material as well. Fluorescent spectra of **R-NH₂** in toluene and DMF were determined and shown in **Fig. S1**, indicating a blue-shift in solution with respect to the solid samples. Meanwhile, the AIE characteristic of **R-NH₂** has been conducted (**Fig. S2**), demonstrating the existence of AIE feature for **R-NH₂**.

To determine the mechanism of the mechanofluorochromic compound, DSC measurements and IR spectra were conducted. Reproducible heating DSC result (**Fig. 3A**) showed that the original state of **R-NH₂** had an endothermic peak located at 176 °C with enthalpy value 3.0 kJ mol⁻¹, which indicated a melting transition. Whereas for the grinding state of the compound, the endothermic

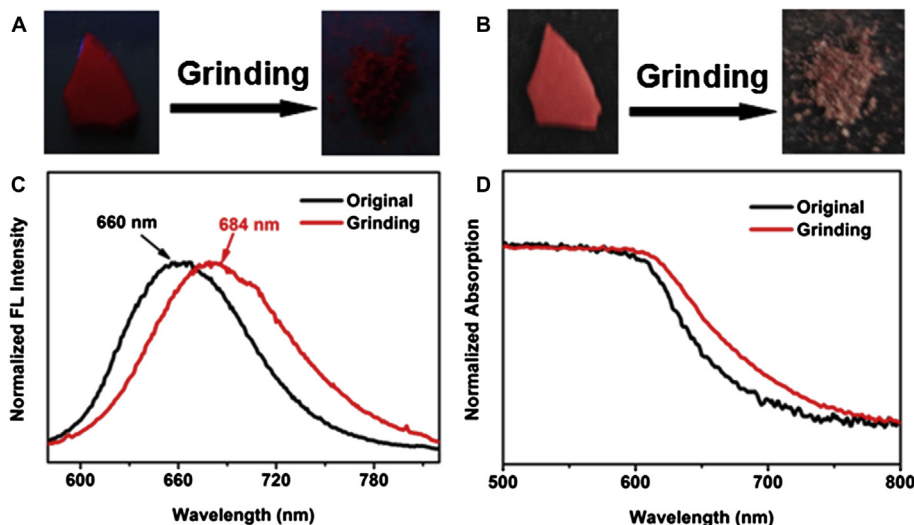


Fig. 2. A. Fluorescent image of **R-NH₂** before and after grinding when taken at room temperature under 365 nm UV light; B. image of **R-NH₂** before and after grinding when taken at room temperature under daylight; C. normalized solid-state fluorescent spectra of **R-NH₂** in original and grinding states; D. normalized solid-state UV–vis spectra of **R-NH₂** in original and grinding states.

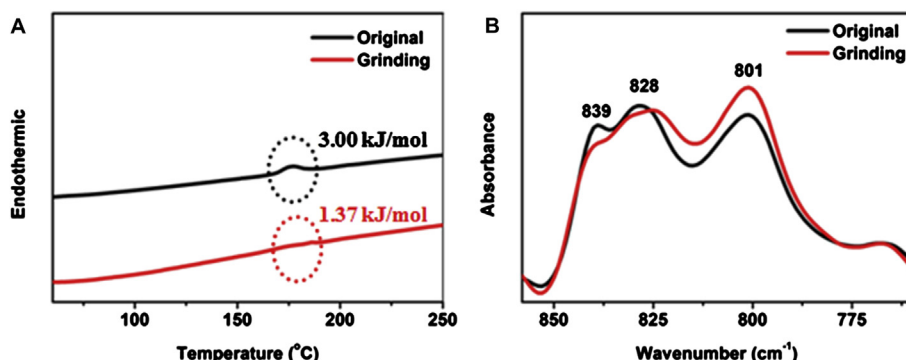


Fig. 3. A. DSC curves of **R-NH₂** in original and grinding states; B. IR spectra of **R-NH₂** in original and grinding states, the absorption is normalized according to the C–H stretching band at 2924 cm⁻¹.

peak located at 176 °C greatly decreased, with enthalpy value reduced to 1.37 kJ mol⁻¹. This result suggested that destruction of the crystalline structure was a direct cause of mechanofluorochromism of **R-NH₂**.⁹ More detailed information is provided by IR spectra (Fig. 3B). The strong absorption signals at 839, 828, and 801 cm⁻¹ emerged in the original sample of **R-NH₂**. When the original sample was ground, both IR absorption signals at 839 and 828 cm⁻¹ decreased, whereas the absorption position at 801 cm⁻¹ dramatically increased, which were ascribed to the changes of C–H out-of-plane bending vibration bands in aryl group of the compound. The IR results further indicated the mechanism of mechanofluorochromism was caused by the destruction of aggregation state owing to the changes of C–H bending vibrations in aryl groups of **R-NH₂**.

To test the reproducibility of the ground state compound, the ground sample was fumed by dichloromethane solvent in a sealed beaker for 10 min to obtain the resulting recovered sample. Then solid-state fluorescent spectrum of the recovered sample was carried out (Fig. 4A). The fluorescent wavelength moved from 684 nm of the ground sample to 660 nm, indicating good reversibility. This result demonstrated that the destruction of crystalline structure of **R-NH₂** could be easily recovered by solvent fuming, which exhibited important advantage for practical applications of the material with good feasibility. SWAXS measurements were employed to elucidate the microstructures of **R-NH₂** in original, grinding, and recovered states (Fig. 4B). The sharp scattering peaks were observed for the original sample located at 2.54, 3.73, and 18.0 nm⁻¹ (q), indicating an ordered crystalline structure. After grinding, a transition from crystalline structure to amorphous phase occurred with the above sharp peaks attenuated or even disappeared. Finally the recovered sample by solvent fuming led to the recovery of the crystalline structure by accompanying the appearance of peaks that coincided with the original sample. The results indicated that the reversible transition between the ordered and disordered molecular aggregations was crucial for the mechanofluorochromic properties.³¹

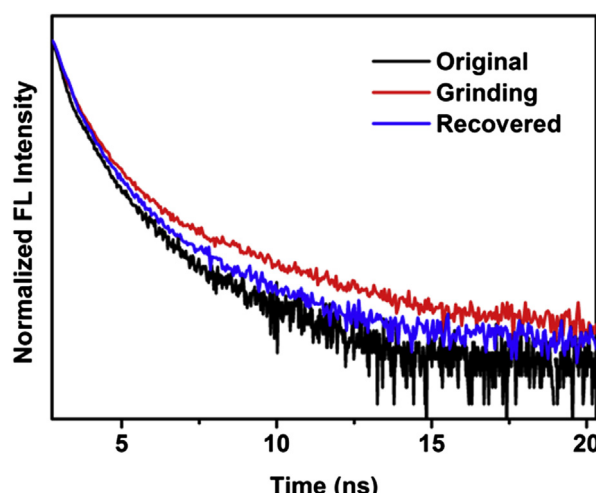


Fig. 5. Time-resolved emission decay curves of **R-NH₂** in original, grinding, and recovered state.

Table 1

Solid-state fluorescence lifetime data of **R-NH₂** in original, grinding and recovered state

Sample	τ_1 (ns) ^a	A_1 ^b	τ_2 (ns) ^a	A_2 ^b	$\langle\tau\rangle$ (ns) ^c
Original	0.35	0.64	1.25	0.36	0.67
Grinding	0.49	0.75	2.16	0.25	0.91
Recovered	0.47	0.78	1.75	0.22	0.75

^a Fluorescence lifetime.

^b Fractional contribution.

^c Weighted mean lifetime.

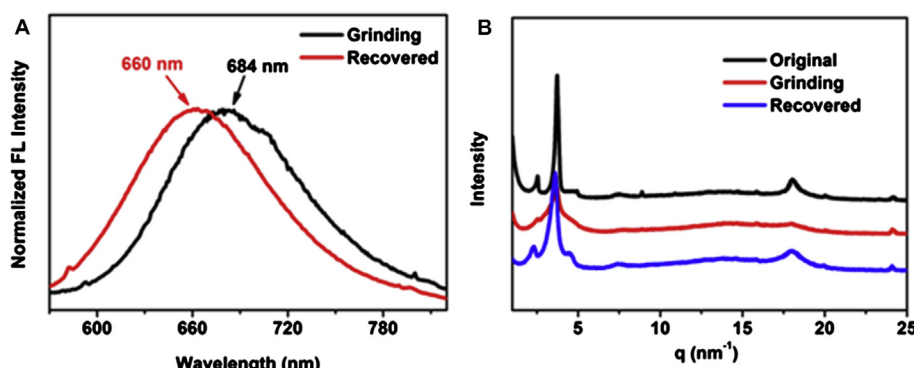


Fig. 4. A. Normalized solid-state fluorescent spectra of **R-NH₂** in grinding and recovered states; B. SWAXS patterns of **R-NH₂** in original, grinding, and recovered states.

The time-resolved emission-decay behaviors of **R-NH₂** in original, grinding, and recovered states were investigated to obtain further information of the mechanofluorochromism. The time-resolved fluorescence curves and the lifetime data are illustrated in Fig. 5 and Table 1, respectively. Two relaxation pathways were shown for the fluorescence decay, indicating that the time-resolved PL spectra of the compound included independent emissions from the segments with different π -conjugation extent due to the detected multiple lifetimes.³² The weighted mean lifetimes $\langle\tau\rangle$ of the original and grinding sample were significantly different: 0.67 ns (original) and 0.91 ns (grinding). After recovered by solvent fuming, the $\langle\tau\rangle$ of the sample reduced to 0.75 ns. The results

indicated that the obvious increasement of lifetime gave rise to the significant changes of fluorescent wavelength.³²

3. Conclusions

In summary, we have synthesized a new cyano-substituted diarylethene derivative (**R-NH₂**) with reversible far-red mechanofluorochromic property. To the best of our knowledge, the 684 nm red-shifted wavelength of the ground **R-NH₂** is the longest wavelength that has appeared in the literature. The mechanofluorochromic mechanism was investigated and ascribed to the destruction of crystalline structure causing the changes of C–H out-

of-plane bending vibrations in aryl group of the compound and the obvious increasement of fluorescence lifetime. The synthetic strategy reported here can be extended to prepare more and more long-wavelength emission mechanofluorochromic materials, which can broaden the scope of application of such materials and for thoroughly understanding the mechanofluorochromic mechanism.

4. Experimental procedure

4.1. Materials and characterization

Thiophene, 3-(bromomethyl)heptane, thiophene-2-carboxylic acid, thionyl chloride, dimethylamine, *n*-butyllithium, stannic chloride, 2-(4-aminophenyl)acetonitrile, tetrabutylammonium hydroxide (0.8 M in methanol) purchased from Alfa Aesar were used as received. All other agents and solvents were purchased from commercial sources and used directly without further purification. Tetrahydrofuran (THF) was distilled from sodium/benzophenone. Ultra-pure water was used in the experiments. The synthetic route of **R-NH₂** was showed in Scheme 2. Intermediates **1**, **2**, and **3** were prepared according to the literature methods.^{59,60}

¹H NMR and ¹³C NMR spectra were measured on a JEOL 400 MHz spectrometer [CDCl₃ as solvent and tetramethylsilane (TMS) as the internal standard]. HRMS was obtained on Shimadzu LCMS-IT-TOF high resolution mass spectrometry. Fluorescence spectra and lifetime were measured on FLS 920 lifetime and steady state spectrometer. The absolute fluorescent quantum yield for the solid samples were measured on a MK-301 EL/PL Measurement Program (Bunkoukeiki Co., Ltd, Japan) equipped with an integrating sphere and a CCD spectrometer (Andor Tech, CCD-6685). Solid-state UV-vis spectra were recorded on a Hitachi U4100 UV-vis-NIR spectrophotometer. Differential scanning calorimetry (DSC) curves were performed on TA Instruments DSC Q2000 at a heating rate of 10 °C min⁻¹ under N₂ atmosphere. The FT-IR spectra were obtained in a transmission mode on a Perkin–Elmer Spectrum 100 spectrometer (Waltham, MA, USA). Typically, 8 scans at a resolution of 1 cm⁻¹ were accumulated to obtain one spectrum. 1D small and wide angle X-ray scattering (SWAXS) experiments were carried out with a SAXS instrument (SAXSess, Anton Paar) containing Kratky block-collimation system. An image plate was used to record the scattering patterns form from 0.06 to 29 nm⁻¹.

4.2. Synthesis of intermediate 4

Compound **3** (458 mg, 0.79 mmol) was dissolved in anhydrous THF (40 mL) under Ar gas, then the temperature of the solution was cooled to –78 °C, afterward, 0.79 mL *n*-BuLi (2.5 mol/L in THF) was added, allowing the mixture to react for 1 h with the temperature raising to room temperature, and then cooled to –78 °C again, 0.3 mL DMF was added dropwise to the solution for 0.5 h, the solution was stirred at room temperature for 3 h, then water was added to quench the reaction. The resulting mixture was extracted by dichloromethane, purification was carried out by column chromatography on silica gel using petroleum ether–dichloromethane (2:1, v/v) as the eluent to obtain pure compound **4** as orange-red solid (0.35 g, yield 70%). ¹H NMR (400 MHz, CDCl₃) δ (ppm): 0.89–1.00 (m, 12H, –CH₃), 1.29–1.49 (m, 16H, –CH₂–), 1.62–1.78 (m, 2H, (methylene)₃C–H), 2.89 (d, 4H, *J*=6.8 Hz, thiienyl–CH₂–), 6.95 (d, 2H, *J*=3.6 Hz, thiienyl–H), 7.34 (d, 2H, *J*=3.6 Hz, thiienyl–H), 8.36 (s, 2H, thiienyl–H), 10.10 (s, 2H, –CHO); HRMS calcd for C₃₆H₄₂O₂S₄, [M+H]⁺: 635.2140, found 635.2138.

4.3. Synthesis of R-NH₂

A solution of **4** (0.35 g, 0.55 mmol) and 2-(4-aminophenyl)acetonitrile (0.20 g, 1.50 mmol) in ethanol (20 mL) was stirred at

room temperature. Then tetrabutylammonium hydroxide solution (0.8 M, 10 drops) was added and the mixture was heated to reflux for 2 h precipitating a dark red solid. The reaction mixture was cooled to room temperature and filtered, washed with ethanol for several times obtaining a dark red solid **R-NH₂** (0.34 g, yield 71%). ¹H NMR (400 MHz, CDCl₃) δ (ppm): 0.88–0.98 (m, 12H, –CH₃), 1.28–1.42 (m, 16H, –CH₂–), 1.65–1.74 (m, 2H, (methylene)₃C–H), 2.86 (d, 4H, *J*=6.4 Hz, thiienyl–CH₂–), 6.68 (d, 4H, *J*=8.8 Hz, aryl–H), 6.90 (d, 2H, *J*=3.2 Hz, aryl–H), 7.33 (d, 2H, *J*=3.2 Hz, aryl–H), 7.42–7.53 (m, 6H, aryl–H), 7.96 (s, 2H, aryl–H); ¹³C NMR (100 MHz, CDCl₃) δ (ppm): 147.8, 146.6, 139.9, 137.0, 136.1, 130.9, 129.2, 128.4, 127.4, 125.9, 124.5, 123.9, 115.2, 111.2, 41.5, 34.4, 32.5, 29.0, 25.7, 23.1, 14.3, 11.0; IR (cm⁻¹): 3375, 2955, 2924, 2856, 2330, 2212, 1672, 1604, 1581, 1516, 1456, 1377, 1294, 1268, 1234, 1182, 1143, 1076, 839, 828, 801; HRMS calcd. for C₅₂H₅₄N₄S₄, [M+2H]²⁺: 432.1688, found 432.1683.

Acknowledgements

This research was supported by the National Science Foundation of China (No. 21134004, 21201108), and the National 973 Project (No. 2011CB935700), China Postdoctoral Science Foundation (2013T60100, 2012M520243, 2012M520388, 2013T60178).

Supplementary data

Electronic Supplementary data (ESI) available: fluorescent spectra of **R-NH₂** in toluene and DMF; the AIE characteristic of **R-NH₂**. Supplementary data related to this article can be found at <http://dx.doi.org/10.1016/j.tet.2013.10.066>.

References and notes

- Chi, Z.; Zhang, X.; Xu, B.; Zhou, X.; Ma, C.; Zhang, Y.; Liu, S.; Xu, J. *Chem. Soc. Rev.* **2012**, *41*, 3878–3896.
- Ciardelli, F.; Ruggeri, G.; Pucci, A. *Chem. Soc. Rev.* **2013**, *42*, 857–870.
- Löwe, C.; Weder, C. *Adv. Mater.* **2002**, *14*, 1625–1629.
- Sagara, Y.; Mutai, T.; Yoshikawa, I.; Araki, K. *J. Am. Chem. Soc.* **2007**, *129*, 1520–1521.
- Sagara, Y.; Kato, T. *Nat. Chem.* **2009**, *1*, 605–610.
- Kunzelman, J.; Kinami, M.; Crenshaw, B. R.; Protasiewicz, J. D.; Weder, C. *Adv. Mater.* **2008**, *20*, 119–122.
- Ooyama, Y.; Harima, Y. *J. Mater. Chem.* **2011**, *21*, 8372–8380.
- Sagara, Y.; Kato, T. *Angew. Chem., Int. Ed.* **2008**, *120*, 5253–5256.
- Zhang, X.; Chi, Z.; Li, H.; Xu, B.; Li, X.; Zhou, W.; Liu, S.; Zhang, Y.; Xu, J. *Chem. –Asian J.* **2011**, *6*, 808–811.
- Luo, J.; Xie, Z.; Lam, J. W. Y.; Cheng, L.; Chen, H.; Qiu, C.; Kwok, H. S.; Zhan, X.; Liu, Y.; Zhu, D.; Tang, B. Z. *Chem. Commun.* **2001**, 1740–1741.
- An, B.-K.; Kwon, S.-K.; Jung, S.-D.; Park, S. Y. *J. Am. Chem. Soc.* **2002**, *124*, 14410–14415.
- Zhang, X.; Yang, Z.; Chi, Z.; Chen, M.; Xu, B.; Wang, C.; Liu, S.; Zhang, Y.; Xu, J. *J. Mater. Chem.* **2010**, *20*, 292–298.
- Zhang, X.; Chi, Z.; Li, H.; Xu, B.; Li, X.; Liu, S.; Zhang, Y.; Xu, J. *J. Mater. Chem.* **2011**, *21*, 1788–1796.
- Zhang, X.; Chi, Z.; Zhang, Y.; Liu, S.; Xu, J. *J. Mater. Chem. C* **2013**, *1*, 3376–3390.
- Zhang, X.; Chi, Z.; Xu, B.; Li, H.; Yang, Z.; Li, X.; Liu, S.; Zhang, Y.; Xu, J. *Dyes Pigm.* **2011**, *89*, 56–62.
- Zhang, X.; Chi, Z.; Xu, B.; Li, H.; Zhou, W.; Li, X.; Zhang, Y.; Liu, S.; Xu, J. *J. Fluoresc.* **2011**, *21*, 133–140.
- Chen, C.; Liao, J.-Y.; Chi, Z.; Xu, B.; Zhang, X.; Kuang, D.-B.; Zhang, Y.; Liu, S.; Xu, J. *J. Mater. Chem.* **2010**, *22*, 8994–9005.
- Zhang, X.; Zhang, X.; Wang, S.; Liu, M.; Zhang, Y.; Tao, L.; Wei, Y. *Nanoscale* **2013**, *5*, 147–150.
- Zhang, X.; Zhang, X.; Wang, S.; Liu, M.; Zhang, Y.; Tao, L.; Wei, Y. *ACS Appl. Mater. Interfaces* **2013**, *5*, 1943–1947.
- Zhang, X.; Zhang, X.; Wang, S.; Liu, M.; Zhang, Y.; Tao, L.; Wei, Y. *RSC Adv.* **2013**, *3*, 9633–9636.
- Zhang, X.; Zhang, X.; Yang, B.; Liu, M.; Liu, W.; Chen, Y.; Wei, Y. *Polym. Chem.* **2013**, *4*, 4317–4321.
- Li, X.; Zhang, X.; Chi, Z.; Chao, X.; Zhou, X.; Zhang, Y.; Liu, S.; Xu, J. *Anal. Methods* **2012**, *4*, 3338–3343.
- Zhang, X.; Liu, M.; Yang, B.; Zhang, X.; Chi, Z.; Liu, S.; Xu, J.; Wei, Y. *Polym. Chem.* **2013**, *4*, 5060–5064.
- Zhang, X.; Liu, M.; Yang, B.; Zhang, X.; Chi, Z.; Liu, S.; Xu, J.; Wei, Y. *Colloids Surf., B* **2013**, *112*, 81–86.
- Zhang, X.; Zhang, X.; Yang, B.; Hui, J.; Liu, M.; Chi, Z.; Liu, S.; Xu, J.; Wei, Y. *Polym. Chem.* **2014**, , <http://dx.doi.org/10.1039/C3PY01143G>

26. Zhang, X.; Zhang, X.; Yang, B.; Liu, M.; Liu, W.; Chen, Y.; Wei, Y. *Polym. Chem.* **2014**, , <http://dx.doi.org/10.1039/C3PY00984J>
27. Zhang, X.; Zhang, X.; Yang, B.; Zhang, Y.; Liu, M.; Liu, W.; Chen, Y.; Wei, Y. *Colloids Surf., B* **2013**, , <http://dx.doi.org/10.1016/j.colsurfb.2013.09.031>
28. Li, X.; Chi, Z.; Xu, B.; Li, H.; Zhang, X.; Zhou, W.; Zhang, Y.; Liu, S.; Xu, J. *J. Fluoresc.* **2011**, *21*, 1969–1977.
29. Chen, C.; Liao, J.-Y.; Chi, Z.; Xu, B.; Zhang, X.; Kuang, D.-B.; Zhang, Y.; Liu, S.; Xu, J. *RSC Adv.* **2012**, *2*, 7788–7797.
30. Yang, Z.; Yu, T.; Chen, M.; Zhang, X.; Wang, C.; Xu, B.; Zhou, X.; Liu, S.; Zhang, Y.; Chi, Z.; Xu, J. *Acta Polym. Sin.* **2009**, *560*–565.
31. Zhang, X.; Chi, Z.; Xu, B.; Chen, C.; Zhou, X.; Zhang, Y.; Liu, S.; Xu, J. *J. Mater. Chem.* **2012**, *22*, 18505–18513.
32. Zhang, X.; Chi, Z.; Zhou, X.; Liu, S.; Zhang, Y.; Xu, J. *J. Phys. Chem. C* **2012**, *116*, 23629–23638.
33. Zhang, X.; Chi, Z.; Zhang, J.; Li, H.; Xu, B.; Li, X.; Liu, S.; Zhang, Y.; Xu, J. *J. Phys. Chem. B* **2011**, *115*, 7606–7611.
34. Zhou, X.; Li, H.; Chi, Z.; Xu, B.; Zhang, X.; Zhang, Y.; Liu, S.; Xu, J. *J. Fluoresc.* **2012**, *22*, 565–572.
35. Zhang, X.; Chi, Z.; Xu, B.; Jiang, L.; Zhou, X.; Zhang, Y.; Liu, S.; Xu, J. *Chem. Commun.* **2012**, *10895*–10897.
36. Zhou, X.; Li, H.; Chi, Z.; Zhang, X.; Zhang, J.; Xu, B.; Zhang, Y.; Liu, S.; Xu, J. *New J. Chem.* **2012**, *36*, 685–693.
37. Chi, Z.; He, K.; Li, H.; Zhang, X.; Xu, B.; Liu, S.; Zhang, Y.; Xu, J. *Chem. J. Chin. Univ.* **2012**, *33*, 725–731.
38. Bu, L.; Sun, M.; Zhang, D.; Liu, W.; Wang, Y.; Zheng, M.; Xue, S.; Yang, W. *J. Mater. Chem. C* **2013**, *1*, 2028–2035.
39. Wang, Y.; Liu, W.; Bu, L.; Li, J.; Zheng, M.; Zhang, D.; Sun, M.; Tao, Y.; Xue, S.; Yang, W. *J. Mater. Chem. C* **2013**, *1*, 856–862.
40. Qi, Q.; Liu, Y.; Fang, X.; Zhang, Y.; Chen, P.; Wang, Y.; Yang, B.; Xu, B.; Tian, W.; Zhang, S. X.-A. *RSC Adv.* **2013**, *3*, 7996–8002.
41. Dong, Y. Q.; Li, C.; Luo, X.; Zhao, W.; Li, C.; Liu, Z.; Bo, Z.; Dong, Y.; Tang, B. Z. *New J. Chem.* **2013**, *37*, 1696–1699.
42. Shan, G.-G.; Li, H.-B.; Qin, J.-S.; Zhu, D.-X.; Liao, Y.; Su, Z.-M. *Dalton Trans.* **2012**, *41*, 9590–9593.
43. Zhao, N.; Yang, Z.; Lam, J. W.; Sung, H. H.; Xie, N.; Chen, S.; Su, H.; Gao, M.; Williams, I. D.; Wong, K. S. *Chem. Commun.* **2012**, *8637*–8639.
44. Luo, X.; Zhao, W.; Shi, J.; Li, C.; Liu, Z.; Bo, Z.; Dong, Y. Q.; Tang, B. Z. *J. Phys. Chem. C* **2012**, *116*, 21967–21972.
45. Wei, R.; Song, P.; Tong, A. *J. Phys. Chem. C* **2013**, *117*, 3467–3474.
46. Teng, M.-J.; Jia, X.-R.; Chen, X.-F.; Wei, Y. *Angew. Chem., Int. Ed.* **2012**, *51*, 6398–6401.
47. Yuan, W. Z.; Tan, Y.; Gong, Y.; Lu, P.; Lam, J. W.; Shen, X. Y.; Feng, C.; Sung, H. H.-Y.; Lu, Y.; Williams, I. D. *Adv. Mater.* **2013**, *25*, 2837–2843.
48. Wang, J.; Mei, J.; Hu, R.; Sun, J. Z.; Qin, A.; Tang, B. Z. *J. Am. Chem. Soc.* **2012**, *134*, 9956–9966.
49. Ooyama, Y.; Oda, Y.; Hagiwara, Y.; Fukuoka, H.; Miyazaki, E.; Mizumo, T.; Ohshita, J. *Tetrahedron* **2013**, *69*, 5818–5822.
50. Kwon, M. S.; Gierschner, J.; Yoon, S.-J.; Park, S. Y. *Adv. Mater.* **2012**, *24*, 5487–5492.
51. Shi, C.; Guo, Z.; Yan, Y.; Zhu, S.; Xie, Y.; Zhao, Y. S.; Zhu, W.; Tian, H. *ACS Appl. Mater. Interfaces* **2013**, *5*, 192–198.
52. Liu, W.; Wang, Y.; Sun, M.; Zhang, D.; Zheng, M.; Yang, W. *J. Chem. Commun.* **2013**, *6042*–6044.
53. Wang, Y.; Li, M.; Zhang, Y.; Yang, J.; Zhu, S.; Sheng, L.; Wang, X.; Yang, B.; Zhang, S. X.-A. *Chem. Commun.* **2013**, *6587*–6589.
54. Rao, M. R.; Liao, C.-W.; Su, W.-L.; Sun, S.-S. *J. Mater. Chem. C* **2013**, *1*, 5491–5501.
55. Rao, M. R.; Liao, C.-W.; Sun, S.-S. *J. Mater. Chem. C* **2013**, *1*, 6386–6394.
56. Qi, Q.; Fang, X.; Liu, Y.; Zhou, P.; Zhang, Y.; Yang, B.; Tian, W.; Zhang, S. X.-A. *RSC Adv.* **2013**, *3*, 16986–16989.
57. Ooyama, Y.; Sugiyama, T.; Oda, Y.; Hagiwara, Y.; Yamaguchi, N.; Miyazaki, E.; Fukuoka, H.; Mizumo, T.; Harima, Y.; Ohshita, J. *Eur. J. Org. Chem.* **2012**, *2012*, 4853–4859.
58. Frisch, M. J.; Trucks, G. W.; Schlegel, H. B. *Gaussian 03, Revision D.01; Gaussian: Wallingford, CT*, 2004.
59. Ellinger, S.; Ziener, U.; Thewalt, U.; Landfester, K.; Möller, M. *Chem. Mater.* **2007**, *19*, 1070–1075.
60. Huo, L.; Zhang, S.; Guo, X.; Xu, F.; Li, Y.; Hou, J. *Angew. Chem., Int. Ed.* **2011**, *123*, 9871–9876.